Hydrophobic and Flame-Retardant Foam Based on Cellulose

Amal H. Abdel Kader
National Research Centre
sawsan Dacrory
National Research Centre
Tawfik A. Khattab
National Research Centre
samir kamel (samirki@yahoo.com)
National Research Center https://orcid.org/0000-0002-7971-4318
Hussein Abou-Yousef
National Research Centre

Research Article

Keywords: Cellulosic Foam, Dolomite, Silicon rubber, Anti-inflammability, Superhydrophobic.

Posted Date: August 17th, 2021

DOI: https://doi.org/10.21203/rs.3.rs-758869/v1

Version of Record: A version of this preprint was published at Journal of Polymers and the Environment on January 4th, 2022. See the published version at https://doi.org/10.1007/s10924-021-02355-4.

Abstract

A series of lightweight, hydrophobic, and fire retardant foams were fabricated through activation of cellulose by phosphoric acid as a primarily step. Dolomite clay was embedded onto the cellulosic suspensions with gelatin/ tannin as adhesive followed by freeze drying process. A solution of the environmentally friendly silicone rubber (RTV) was applied onto foam samples via spray-coating to improve their water repealing performance, which was explored by investigating both of water contacting angle and wettability time of the coated foam samples. Flammability characteristics, thermal decomposition, surface morphology, and chemical structure of treated and untreated foams were investigated by flammability test, thermogravimetric analysis, scanning electron microscopy, X-ray diffraction, and Fourier-transform infrared, respectively. Results showed that the foams loaded dolomite and coated RTV have high hydrophobicity as well as anti-inflammability.

Introduction

Cellulose and its derivatives have various and important applications in a wide range of fields, such as textiles, paper industry, medicine, ink, and paints.[1–4]. The development of fire retardant cellulosic materials has received attention due to conflagration that causing massive losses for society. Fire retardant cellulosic materials have been manufactured based on blending and chemical surface modifications [3, 5, 6].

Recently, the manufacturing of foam materials is a big target, especially from natural and renewable resources [7]. The foam materials exhibit unique properties such as low density, high porosity, high specific surface area, and high thermal insulation [8]. Cellulosic materials are promising for manufacture functional foams and aerogels to replace petroleum-based foam products. The preparation of cellulosic foam is dependent on the combination of cellulose substrate with inorganics materials e.g., clays, oxides [9] or/and organics e.g. carbon nanotubes, graphene oxide[10]. The varieties of such combinations can produce various hybrid foam composites having distinctive properties with specific functionalities such as high compressive strength [11], thermal insulation[7], magnetic and conducting properties[11]. When it comes to the industrial production of such hybrid foams, the number of incorporated components and their origin play an important role. Indeed, using as few as possible components particularly coming from abundant natural resources would effectively simplify the processing conditions and give rise to sustainable material concepts[12].

Freeze-drying is a promising technique to obtain well-oriented and highly porous aerogels. Where the unidirectional freezing of the aqueous suspension enables the ice crystals to grow along the temperature decreasing gradient resulting in a highly aligned porous structure by sublimation. The porosity of foam material can be controlled by the cooling rate since a higher cooling rate led to smaller pores [13, 14].

An important disadvantage of cellulosic foam is low fire resistance due to the presence of (C, H, and O) in the cellulose structures that help to start combustion. Also, the available highly distributed hydroxyl

groups can catch the fire leading to its poor thermal stability [15]. The free hydroxyl groups along make hydrophilic properties for the cellulose chain. The association of water molecules with cellulose enhances the chemical degradation resulting in decreasing the mechanical performance due to the collapse of the cell structure of foam [16]. The efficiency of fire resistance cellulosic foam is affected by fibers' crystallinity and orientation. The higher cellulose crystallinity results in higher levels of levoglucosan during the pyrolysis and hence increases the flammability. While increasing the cellulosic fiber orientation could decrease the pyrolysis rate and therefore decrease the flammability [17].

On the other hand, clay nano-particles embedded in the cellulosic foam can contribute to the fire retardant properties of foam due to reducing heat transfer and catalyzing the char formation from cellulose due to the presence of metal ions in the chemical structure of clay. Recently, the flame retardant properties of cellulose-based freeze casting foam are enhanced by TEMPO modification of cellulose substrate in blending with boric acid and sepiolite clay (a micro fibrous magnesium silicate). The increasing efficiency of the flame retardant properties of the formed foam was attributed to the crosslinking among the main cellulosic macromolecules due to the presence of borate anions and clay. Consequently, the char oxidation process could be shifted to a higher temperature resulting in reducing in the formation of combustible volatile materials such as leuvoglucosane [18].

The development of water-repellent surfaces, with a sliding angle < 10° and a contacting angle > 150°, has been recently an important research field for a variety of applications, such as self-cleaning, and antifouling purposes[19]. Both nano- and micro-hierarchical morphologies can introduce surface roughness as outstanding heuristic models to achieve a hydrophobic character. Nonetheless, the surface energy based materials are usually fluorine-containing agents, which are highly poisonous and expensive[19]. There have been several chemical and physical methods that have been reported for the development of hydrophobic surfaces, such as electrospun and self-assembled nanofibers, sol-gel, lithography, as well as chemical and plasma etching. Nonetheless, those methods are typically time-consuming, costly, and usually necessitate multiple-step complicated processing and instruments[20]. The spray-coating method has been applied as an easy and cheap method for the development of functional surfaces at room temperature [21]. Room temperature vulcanized (RTV) silicone is a category of eco-friendly polymers with the ability to cure at room temperature in the presence of a catalytic amount of dibutyltin dilaurate. RTV exhibits high resistance to chemicals, acids and bases, ageing and high temperatures. It is characterized with excellent thermal stress and mechanical properties, low shrinking, as well as low viscosity and high hardness. These properties made it applicable in different fields, such as aviation and electronics [22, 23].

The study aimed to prepare a fire retarding composite from phosphorylated cellulose blended with dolomite clay in form of foam by using gelatin/ tannin as adhesive. Loading of silicon rubber to enhance the water repealing and fire retarding also was studied. Characterization of foam composites could be investigated by using FTIR, SEM, EDX, TGA, hydrophobic measurements, and flammability properties.

Materials And Methods

Materials

The cellulose-based material used was kraft bleached bagasse pulp, which was consisting of lignin 0.37%, hemicelluloses 22%, and α-cellulose 85%. Ortho-phosphoric acid 85% (wt/wt) (al-Nasr chemical Co.) was used for pulp pretreatment. Dolomite clay was delivered from Ataka Mountain, Egypt. In order to enhance the strength of the foam sample, gelatin powder (delivered from Alex. Chemical Co.) and tannin (Sigma-Aldrich) were used. RTV-2540 Decoseal was obtained from ADMICO, Egypt.

Phosphoric acid treatment

In order to defibrillation, bleached bagasse pulp (50 g dried weight) was soaked in distilled water at a liquor ratio of 1: 10 with continuous stirring for one hour. The produced suspension pulp was de-watering by G2 sintered glass until obtaining pulp with consistency 1:4 (included with 200 ml distilled water). The defibrillated produced pulp was treated with phosphoric acid (50 % wt/wt). The addition of concentrated ortho-phosphoric acid (85 % wt/ wt) to the defibrillated pulp was based on the amount of water associated with the pulp to produce finally 50 g pulp immersed in 50 % phosphoric acid with liquor ratio 1: 7. The suspended pulp in phosphoric acid was agitation at 50 ^{o}C for six hours followed by washing with distilled water giving activated cellulose [24].

Preparation of cellulose-based foam

A typical experiment for foam preparation was performed as follows: 4 g dried weight phosphorylated pulp was suspended in 100 ml distillated water via stirring in a glass beaker using mechanical stirring. 0.4 g of gelatin was dissolved in 10 ml distilled water, and then 0.2 g tannin was mixed with gelatin solution via stirring till complete dissolution. The mixture of gelatin/tannin was added to the pulp suspension with continuous stirring and sodium bicarbonate was added. Different amounts of dolomite clay(0.0, 0.5, 1.5, 2 and 3g)were added to the pulp suspension after blending with gelatin/tannin mixture in order to obtain finally a suspension composite constituents phosphorylated pulp/gelatin/tannin-dolomite and coded as F1, F2, F3, F4, and F5 respectively. The suspension was poured into Petri dish and frozen in a deep-freezer at − 80°C followed by the freeze-drying process (ALPHA 1–2/LD PLUS, Martin Christ, Germany) to afford a foam.

Preparation of superhydrophobic foams

Solution of RTV in petroleum ether (15 g/L) was stirred for 60 minutes; and then subjected to ultrasonic at 35 kHz for 60 minutes to guarantee the formation of a homogeneous solution. The foam samples were then spray-coated using the above prepared solution, and then air-dried for 15 minutes to afford samples FS1, FS2, FS3, FS4, and FS5 depending on the total content of dolomite clay.

Foam characterization

Density and porosity

The density of cellulose-based aerogels/foams is between 10 and 10.5 kg/m^3. Weight and volume can measure the density of aerogels by dividing the weight by the volume. The porosity can be evaluated from the density of the aerogels (ρ∗) by utilizing the following equation:

$$Porosity\ \% = 1 - \frac{\rho *}{\rho c}$$

where the ratio ρ∗/ρ_c is the relative density. The density of cellulose (ρ_c) is assumed to be 1460 kg/m^3 [25].

FT-IR spectra were recorded in the range of 400–4000 cm^{-1}on (Shimadzu 8400S) FT-IR Spectrophotometer. The XRD patterns were investigated on a Diano X-ray diffractometer using CoKα radiation source energized at 45 kV and a Philips X-ray diffractometer (PW 1930 generator, PW 1820 goniometer) with CuK radiation source (λ = 0.15418 nm), at a diffraction angle range of 2θ from 10 to 70° in reflection mode. The thermal stability was carried out using a TGA Perkin-Elmer (STA6000), with a heating rate (10ºC/min). The temperature ranged from room temperature up to 900 ºC under air atmosphere. The chemical composition of dolomite was also determined using sequential advanced AXIOS wavelength-dispersive X-ray fluorescence (WDXRF).

The surface morphology of cellulose and foam with different concentrations of dolomite were analyzed using electron microscope FEI IN SPECTS Company, Philips, Holland, environmental scanning without coating. The microscope was attached to a dispersive energy spectrometer (EDX). The images were obtained using an accelerating voltage of 10-15kV. EDX analysis was carried out to be supporting information confirming the presence of clay in the prepared composites.

Hydrophobic measurements; both of slide and water contacting angles, as well as wettability time[26] of the spray-coated foam samples were determined under ASTM(D-7334) standard test using DataphysicsOCA15EC (Germany).

The flame test of the spray-coated foam samples was carried out under standard BS5438(1989) test[27].

Result And Discussion

Preparation of foams

Phosphoric acid was used to make decrystalization of cellulosic pulp to be more swollen and the treatment of pulp was performed by phosphoric acid includes two main processes[28]. Firstly, an esterification reaction between hydroxyl groups of cellulose and phosphoric acid to form cellulose phosphate (H_3PO_4 + cellulose → cell-O-PO_3H_2). Secondary, a competition of hydrogen-bond formation between hydroxyl groups of cellulose chains and hydrogen-bond formation between one hydroxyl group of a cellulose chain and a water molecule or with hydrogen ions. Meanwhile, another by-reaction, acid hydrolysis of β-glucosidic bonds of cellulose will take place. However, such acid hydrolysis could be

overcome by decreasing the dissolution temperature. The freeze-drying approach has been adopted to prepare cellulose-based composite foam by blending pulp with dolomite clay micro-particles at different loading ratios. Upon freeze-drying, strong anisotropic aerogel was produced that may resist combustion and exhibited a low thermal conductivity. During the freeze-drying process, cellulose nanofibrils align laterally and form layer structures of varying lengths due to the diffusion forces or inter-fibrillar hydrogen bonding. Partial decomposition of sodium bicarbonate added during the preparation of foams, resulted in the formation of carbon dioxide that enhanced pores formation in the pulp matrix.

There are different techniques can be used to detect the elemental content of the material. One of these is the wavelength-dispersive X-ray fluorescence (WDXRF) which is generally affords a detection limit of elements with a total content higher than 10 mg/kg. The elemental composition of dolomite was carried out using WDXRF which indicated that the main constitutes are CaO and MgO with 27.85 and 15.94 % respectively which is compatible with the chemical structure of dolomite (**Fig. 1**). The moisture and volatile material, water and carbon dioxide from carbonates that present in the sample represent 39.39 % (**Table 1**).

Morphology studies

Porosity is an important feature of aerogel structure since it determines the effective volume of air in the matrix. As shown in **Fig. 2a**, cellulosic pulp has organized fibrils layered structure. Fibrils are highly interconnected leading to dense aerogel structure with macro-pores at the surface of foam. **Fig. 2b-d**, illustrated SEM for composite foams that comprised from phosphate cellulose pulp blended with different ratios of dolomite clay. Generally, the outer surface of these composites exhibited a smooth 2D sheet like structure with few macro-pores. The loading concentrations of dolomite upon the outer surface of fibrils have confirmed by EDX that showed increasing the concentrations Mg and Ca representing the main constituents of dolomite. On the other hand, the concentration of P was approximately the same for composites sample as in **Fig. 2b-d**. At the highest concentration of dolomite clay **Fig. 2d**, the aerogel structure collapsed, forming a microstructure composed of smaller pores.

The presence of high concentration of dolomite particles near cellulose fibrils may have hindered the inter-fibrillar attraction, hence causing disruption of the fibril layer structure. The adhesive system components, tannin and gelatin, added to blended composite of pulp and dolomite has important role in case of such high loading of clay. The adhesive system enabled the connectivity of the fibril layer structure to be still preserved, maintaining physical integrity of aerogel. The dolomite particles have occupied the matrix pores in case of highest dolomite concentration, while partial occupation of matrix pores has been achieved in case of low dolomite concentration. This agrees with the lowest porosity and highest density values of produced foam at highest concentration of dolomite, while lowest density and highest porosity could be obtained in case of lowest concentration of dolomite (**Table 2**).

Fig. 3 illustrated SEM for blended composites of cellulosic pulp and dolomite after treatment with silicone rubber for acquiring the composites water repelling properties. The accumulation of silicon rubber has appeared as co-centered layered agglomeration on the surface of composite matrix. In case of composite

with low dolomite concentrations, silicon rubber has light distribution on the composite matrix although high Si concentration manifested from EDX data. On the other hand, dense distribution of silicon rubber has obtained in case of composite with highest dolomite concentration, despite of lowest concentration of silicon rubber obtained from EDX data. These anomalous results can be interpreted in view of incompatibility of dolomite and silicon rubber due to their zeta potentials. Low concentration of dolomite in composite matrix enabled silicon rubber to diffuse through the macro-pores and the cavities of the matrix, where high concentration of dolomite hinder diffusion of silicon rubber through the matrix pores. Consequently, the distribution of silicon rubber could exist only upon the external surface of fibrils forming a coating layer as shown in **Fig. 3c**, leaving most of internal pore surface empty. These results agreed with results as in **Table 2**, where the highest porosity and lowest density of foam composite with silicone rubber was obtained in case of highest dolomite concentration. EDX data has confirmed that lowest silicon rubber concentration for foam composite with silicone rubber foams has been obtained in case of highest dolomite concentration. This confirmed that silicone rubber has not diffused through the pores but only coat the external surface of fibrils.

FTIR spectroscopic analysis

Fig. 4 (cellulose and activated cellulose) illustrates typical absorption bands of cellulose, 3340, 2904, 1116, 1054, 896 cm^{-1} that are assigned for OH, C-H, C-C, C-O-C, and β-linkage respectively [30]. The peaks at 1230, and 928 cm^{-1} were referred to P=O and P-OH respectively [28]. Also, P-O-C was assigned at 803 cm^{-1}. The band at 1710 cm^{-1} [28] which is present in the spectra of foams, can be attributed to C=O stretching mode, and is probably due to the oxidation carried out during phosphorylation of cellulosic fibers[31].

Dolomite displays characteristic FT-IR absorption at 3020, 2626, and 730 cm^{-1} [32], which were shifted, as shown in **Fig. 4**, toward 2850, 2450, and 700 cm^{-1} respectively due the physical interactions with cellulosic fibers. As dolomite concentration was increased in the foam sample, the peaks indicated to presence of P were reduced due the shielding effect of dolomite.

Fig. 4 also illustrates the characteristic bands of silicone rubber impeded in the foam matrix consisted of activated cellulose with dolomite. Generally, the absorption peak at 2960 $cm^{-1}$is assigned to stretching vibration of CH_3. The absorption at 1410 cm^{-1} is referred to the vibration mode of CH_2. The absorption peak at 1250 and 860 $cm^{-1}$are corresponding to the bending and rocking vibrations of CH_3.The absorption peak at 1000 cm^{-1} is assigned to the stretching vibration of Si-O-Si on backbone of silicone rubber. The absorption peak at 780 cm^{-1} is the stretching vibration of Si-C[33]. The peaks indicated to cellulose are extremely diminished due to the predominate peaks referred to silicone rubber that diffused through the foam cavities or coated the external surface of cellulose. All of these suggested incorporation of cellulosic matrix with dolomite clay and silicone rubber.

X-ray Diffraction

XRD of dolomite has been shown characteristic peaks at 2θ = 31.5^{o} and 41.5^{o} that referred to CaO and MgO respectively as well as broad band in region around 10^{o} [34]. **Fig. 5** illustrates XRD for composite samples comprised from activated cellulose with various concentrations of dolomite. At low dolomite concentration, the peaks at 2θ = 31 and 41^{o} are quite small and only the broad band around 10^{o} is appeared obviously. The peak appeared around 2θ = 22^{o} is referred to the crystalline portion of cellulose chain. Low intensities peaks characterized for dolomite may be due to the interaction of dolomite cations with cellulose chains and diffusing distribution of dolomite inside pores and the cavities of the foam matrix. Increasing dolomite concentration, the peaks at 2θ = 31 and 41 ^{o} are distinguished.

XRD of pure silicone rubber has main characteristic peak, which is weak due to a poor crystalline nature in silicone rubber[35]. This feature is manifested obviously for cellulose/dolomite/Silicone rubber composite with low dolomite concentration (**Fig. 5**). As dolomite concentration increased in foam matrix, weak peaks of dolomite could be distinguished at 2θ=31 and 41^{o}. These weak intensities could be attributed the scattering and shielding effects caused by silicone rubber that distributed through matrix. In general, the leak of peaks appeared for composite cellulose/dolomite/ silicone may be attributed to thick layer of silicone rubber that interpretation or coating the cellulosic matrix or low content of dolomite composite.

Thermographimetric analysis (TGA)

TGA was used to investigate the thermal degradation behaviors, thermal stability, and residue formation of cellulose, activated cellulose and foams with different ratios of dolomite before and after treatment with silicone rubber (**Fig. 6)**. The pyrolysis is defined by two competitive pathways, the depolymerization of glycosyl units to volatile levoglucosan or dehydration followed by decomposition of the same units to aromatic char, which is the final residue at the end of TGA test [36]. Cellulosic pulp denotes decomposition temperature at 5% weight loss less than that of activated cellulose. The final residue of cellulose pulp is about 8%, while activated cellulose denotes about 20% residue at 500^{o}C. Therefore, activated cellulose has higher thermal stability than that of cellulose pulp. Addition of dolomite to activated cellulose caused multiple changes in its thermal characteristics. As shown in **Fig. 6**, the major decomposition peaks of low dolomite contents have been shifted to lower temperature 350^{o}C, while high dolomite content has been shifted to 220^{o}C. Generally, dolomite acts as catalyst to possible decomposition pathways take place for foam matrix. At low dolomite content the dehydration pathway was predominant, and hence formation of aromatic char was the major end product. At high dolomite content, the catalytic action influenced in dehydration pathway as well as in depolymerization forming volatile levoglucosan end product. Therefore, the residues at low dolomite content F2, and F3 (about 50% at 1000^{o}C) were higher than the residues resulted from high dolomite content matrix (about 20% at 1000^{o}C). Since, the char formation can prevent the matrix from combustion; the increase of char residue is an indication to the flammability resistance. So, a significant increase of the thermal stability of low dolomite (F2 and F3), content have been achieved compared with high dolomite content (F5).

Fig. 6 shows TGA of foam composites consisting of activated cellulose, dolomite, and silicone rubber with different dolomite contents. As shown in **Fig. 6,** composite FS2 has the lowest thermal stability due to majority constituent of synthetic polymer (silicone rubber) blended with pulp in presence low dolomite content. Increasing the dolomite content can enhance the thermal stability. The composite FS3 denotes 55% residue, while composite FS5 denotes 30% residue at 1000 °C. As the char yield of composites without silicone rubber differ significantly from that with silicone rubber, so the polymer /clay system appears to inhibit the thermal degradation of the foam matrix. The mechanism of the polymer/clay system may be explained as follows: firstly, dolomite can catalyze thermal degradation of foam matrix through dehydration reactions that resulted in carboneous materials. Secondly, these carboneous materials can fill the voids of polymer, silicon rubber, that can shield and inhibit further degradation of these carboneous materials into volatile materials. Thus, existence of silicone rubber preserves most of char produced from the catalytic pyrolysis of foam matrix, and consequently the residue product is higher than that of foam without polymer. In light of this visualization, it is possible to explain why FS3 composite produced amount of residue larger than that resulted from FS5. Despite of high content of dolomite, FS5composite has silicone content lower than that of FS3 composite as mentioned before from EDX. Thus, the amount of polymer in FS5 composite is not able to catch all the produced char. Some of this char can further converted into volatile substances resulting in loss of residue char yield.

Hydrophobic characterization

A surface roughness was created on the surface of the foam samples using spray-coating technology of RTV in petroleum ether under ambient conditions. We were able to produce foam samples spray-coated with RTV to result in improved water contacting angles in the range of 97.8-162.4°. On the other hand, the uncoated foam sample displayed very poor hydrophobic properties. There have been diverse techniques that have been previously described in literature to accomplish the creation of a superhydrophobic surface using costly materials, time-consuming processes, as well as complex procedures and instruments[37]. Therefore, the current method can be described as an effective, simple and cheap method to create a superhydrophobic surface without the requirements of sophisticated apparatus. Furthermore, the present simple technique can be applied for the large-scale production of hydrophobic commodities. The contacting angle of the uncoated sample was monitored at 0°. The spray-coated foam samples illustrated higher water contacting and slide angles as depicted in **Table 3**. Once increasing the concentration of dolomite clay, the contacting angle increased from 97.8° (FS1) to 162.4° (FS4). However, the contacting angle then decreased from 162.4° (FS4) to 154.4° (FS5). The wettability time also increased from 20 minutes (FS1) to 45 minutes (FS5). This could be attributed to the enhanced roughness with increasing the concentration of dolomite clay as well as RTV. However, the extremely higher concentrations of dolomite clay in combination with RTV led to completely filling the pores, which negatively resulted in decreasing the surface roughness to result in decreasing the water contacting angle. In addition, the slide angle was determined to assess the hydrophobic efficiency of the spray-coated foam samples. The changes in the wetting performance were attributed to decreasing the slide angle with the increase of dolomite clay concentration. The slide angle decreased from 13° (FS1) to 8°

(FS4) with increasing the concentration of dolomite clay, and then increased from 8° (FS4) to 9° (FS5). Therefore, the slide angle measurements matched with that of the water contacting angles.

Flam Test

The fire retardancy of the prepared foams was tested by determine the char length and wider char length as given in **Table 3**. Untreated cellulose pulp could not pass the flammability examination and was entirely burnt, indicating its poor flame retardancy.

Loading of low and medium concentration of dolomite improve the fire retardancy properties that detected by the char lengths of these foams. Otherwise the highest concentration of dolomite reduced the fire retardancy due to the existence of high dolomite clay increased the rate of heat transfer to cellulosic matrix. Consequently, char length of that sample increases indicating to reducing of fire retardancy property of this sample. This corresponded with results of Gillani et al who suggested that the dolomite clay enhanced the fire performance and could formed dense and continuous char when incorporated as filler in conventional intumescent fire resistive systems [38]. Moreover, the coating of foams by silicone rubber increased their fire retardancies on comparison with uncoated foams. This can be attributed to the formation of a protective layer that can prevent heat transfer from the heat source and prevent oxygen flow to the flammable material and prevent the supply of pyrolysis gases to the material surface also. These results were agreed with that of TGA of foams.

Conclusions

Utilization of dolomite was successfully enhanced the fire retardancy of cellulosic foam at moderate concentration, while the high concentration reduced the fire retardant property due to the high heat transfer. Cellulose –dolomite foams sample was coated by silicon rubber to improve the water repelling and fire retardant properties. So, the simple production of hydrophobic foam was developed via spray-coating under ambient conditions utilizing a solution of RTV demonstrating water contact angles in the range of 97.8-162.4°, while the sliding angles were in the range of 13 – 8°.

Declarations

Acknowledgments

The authors would like to acknowledge the financial and technical support for this research from National Research Centre, Egypt; under grant number 12010303.

Conflict of interest

The authors have no conflicts of interest to declare.

References

[1] A.J. Ragauskas, C.K. Williams, B.H. Davison, G. Britovsek, J. Cairney, C.A. Eckert, W.J. Frederick, J.P. Hallett, D.J. Leak, C.L. Liotta, The path forward for biofuels and biomaterials, science 311(5760) (2006) 484-489.

[2] D. Klemm, B. Heublein, H.P. Fink, A. Bohn, Cellulose: fascinating biopolymer and sustainable raw material, Angewandte chemie international edition 44(22) (2005) 3358-3393.

[3] K.J. Edgar, C.M. Buchanan, J.S. Debenham, P.A. Rundquist, B.D. Seiler, M.C. Shelton, D. Tindall, Advances in cellulose ester performance and application, Progress in polymer science 26(9) (2001) 1605-1688.

[4] J.-m. Zhang, J. Wu, J. Yu, X.-c. Zhang, Q.-y. Mi, J. Zhang, Processing and functionalization of cellulose with ionic liquids, (2017).

[5] N. Read, E. Heighway-Bury, Flameproofing of Textile Fabrics with particular reference to the Function of Antimony Compounds, Journal of the Society of Dyers and Colourists 74(12) (1958) 823-829.

[6] A.W. Frank, D.J. Daigle, S.L. Vail, Chemistry of Hydroxymethyl Phosphorus Compounds: Part III. Phosphines, Phosphine Oxides, and Phosphonium Hydroxides, Textile Research Journal 52(12) (1982) 738-750.

[7] B. Wicklein, A. Kocjan, G. Salazar-Alvarez, F. Carosio, G. Camino, M. Antonietti, L. Bergström, Thermally insulating and fire-retardant lightweight anisotropic foams based on nanocellulose and graphene oxide, Nature nanotechnology 10(3) (2015) 277-283.

[8] M. Hamedi, E. Karabulut, A. Marais, A. Herland, G. Nyström, L. Wågberg, Nanocellulose aerogels functionalized by rapid layer-by-layer assembly for high charge storage and beyond, Angewandte Chemie 125(46) (2013) 12260-12264.

[9] A.E. Donius, A. Liu, L.A. Berglund, U.G. Wegst, Superior mechanical performance of highly porous, anisotropic nanocellulose–montmorillonite aerogels prepared by freeze casting, Journal of the mechanical behavior of biomedical materials 37 (2014) 88-99.

[10] M.M. González del Campo, M. Darder, P. Aranda, M. Akkari, Y. Huttel, A. Mayoral, J. Bettini, E. Ruiz-Hitzky, Functional hybrid nanopaper by assembling nanofibers of cellulose and sepiolite, Advanced Functional Materials 28(27) (2018) 1703048.

[11] M. Wang, I.V. Anoshkin, A.G. Nasibulin, J.T. Korhonen, J. Seitsonen, J. Pere, E.I. Kauppinen, R.H. Ras, O. Ikkala, Modifying native nanocellulose aerogels with carbon nanotubes for mechanoresponsive conductivity and pressure sensing, Advanced materials 25(17) (2013) 2428-2432.

[12] M. Frydrych, C. Wan, R. Stengler, K.U. O'Kelly, B. Chen, Structure and mechanical properties of gelatin/sepiolite nanocomposite foams, Journal of materials chemistry 21(25) (2011) 9103-9111.

[13] T. Köhnke, A. Lin, T. Elder, H. Theliander, A.J. Ragauskas, Nanoreinforced xylan–cellulose composite foams by freeze-casting, Green Chemistry 14(7) (2012) 1864-1869.

[14] M.C. Gutiérrez, M.L. Ferrer, F. del Monte, Ice-templated materials: Sophisticated structures exhibiting enhanced functionalities obtained after unidirectional freezing and ice-segregation-induced self-assembly, Chemistry of Materials 20(3) (2008) 634-648.

[15] F. Carosio, J. Kochumalayil, F. Cuttica, G. Camino, L. Berglund, Oriented Clay Nanopaper from Biobased Components□ Mechanisms for Superior Fire Protection Properties, ACS applied materials & interfaces 7(10) (2015) 5847-5856.

[16] A. Liu, A. Walther, O. Ikkala, L. Belova, L.A. Berglund, Clay nanopaper with tough cellulose nanofiber matrix for fire retardancy and gas barrier functions, Biomacromolecules 12(3) (2011) 633-641.

[17] J. Alongi, M. Ciobanu, G. Malucelli, Sol–gel treatments for enhancing flame retardancy and thermal stability of cotton fabrics: optimisation of the process and evaluation of the durability, Cellulose 18(1) (2011) 167-177.

[18] T. Saito, Y. Nishiyama, J.-L. Putaux, M. Vignon, A. Isogai, Homogeneous suspensions of individualized microfibrils from TEMPO-catalyzed oxidation of native cellulose, Biomacromolecules 7(6) (2006) 1687-1691.

[19] M.S. Abdelrahman, T.A. Khattab, Development of One-Step Water-Repellent and Flame-Retardant Finishes for Cotton, ChemistrySelect 4(13) (2019) 3811-3816.

[20] X.-M. Li, D. Reinhoudt, M. Crego-Calama, What do we need for a superhydrophobic surface? A review on the recent progress in the preparation of superhydrophobic surfaces, Chemical Society Reviews 36(8) (2007) 1350-1368.

[21] T.A. Khattab, S. Mowafi, H. El-Sayed, Development of mechanically durable hydrophobic lanolin/silicone rubber coating on viscose fibers, Cellulose 26(17) (2019) 9361-9371.

[22] G. Wang, A. Li, K. Li, Y. Zhao, Y. Ma, Q. He, A fluorine-free superhydrophobic silicone rubber surface has excellent self-cleaning and bouncing properties, Journal of Colloid and Interface Science 588 (2021) 175-183.

[23] C. Peng, H. Zhang, Z. You, F. Xu, G. Jiang, S. Lv, R. Zhang, H. Yang, Preparation and anti-icing properties of a superhydrophobic silicone coating on asphalt mixture, Construction and Building Materials 189 (2018) 227-235.

[24] S. Dacrory, H. Abou-Yousef, S. Kamel, G. Turky, Development of biodegradable semiconducting foam based on micro-fibrillated cellulose/Cu-NPs, International journal of biological macromolecules 132 (2019) 351-359.

[25] H. Sehaqui, Q. Zhou, L.A. Berglund, High-porosity aerogels of high specific surface area prepared from nanofibrillated cellulose (NFC), Composites science and technology 71(13) (2011) 1593-1599.

[26] T.A. Khattab, A.L. Mohamed, A.G. Hassabo, Development of durable superhydrophobic cotton fabrics coated with silicone/stearic acid using different cross-linkers, Materials Chemistry and Physics 249 (2020) 122981.

[27] A.R. Horrocks, A. Sitpalan, B.K. Kandola, Design and characterisation of bicomponent polyamide 6 fibres with specific locations of each flame retardant component for enhanced flame retardancy, Polymer Testing 79 (2019) 106041.

[28] M. Ghanadpour, B. Wicklein, F. Carosio, L. Wågberg, All-natural and highly flame-resistant freeze-cast foams based on phosphorylated cellulose nanofibrils, Nanoscale 10(8) (2018) 4085-4095.

[29] J. Xie, T. Chen, B. Xing, H. Liu, Q. Xie, H. Li, Y. Wu, The thermochemical activity of dolomite occurred in dolomite–palygorskite, Applied Clay Science 119 (2016) 42-48.

[30] Q.-y. Mi, S.-r. Ma, J. Yu, J.-s. He, J. Zhang, Flexible and transparent cellulose aerogels with uniform nanoporous structure by a controlled regeneration process, ACS Sustainable Chemistry & Engineering 4(3) (2016) 656-660.

[31] M. Ghanadpour, F. Carosio, P.T. Larsson, L. Wågberg, Phosphorylated cellulose nanofibrils: a renewable nanomaterial for the preparation of intrinsically flame-retardant materials, Biomacromolecules 16(10) (2015) 3399-3410.

[32] J. Ji, Y. Ge, W. Balsam, J.E. Damuth, J. Chen, Rapid identification of dolomite using a Fourier Transform Infrared Spectrophotometer (FTIR): A fast method for identifying Heinrich events in IODP Site U1308, Marine Geology 258(1-4) (2009) 60-68.

[33] S.I. Salih, J.K. Oleiwi, H.M. Ali, Modification of silicone rubber by added PMMA and natural nanoparticle used for maxillofacial prosthesis applications, ARPN J. Eng. Appl. Sci 14 (2019) 781-791.

[34] M. Mohammadi, A. Ghaemi, M. Torab-Mostaedi, M. Asadollahzadeh, A. Hemmati, Adsorption of cadmium (II) and nickel (II) on dolomite powder, Desalination and Water Treatment 53(1) (2015) 149-157.

[35] J. Shen, Y. Yao, Y. Liu, J. Leng, Preparation and characterization of CNT films/silicone rubber composite with improved microwave absorption performance, Materials Research Express 6(7) (2019) 075610.

[36] C. Delhom, L. White-Ghoorahoo, S. Pang, Development and characterization of cellulose/clay nanocomposites, Composites Part B: Engineering 41(6) (2010) 475-481.

[37] S.P. Dalawai, M.A.S. Aly, S.S. Latthe, R. Xing, R.S. Sutar, S. Nagappan, C.-S. Ha, K.K. Sadasivuni, S. Liu, Recent advances in durability of superhydrophobic self-cleaning technology: A critical review, Progress in

Organic Coatings 138 (2020) 105381.

[38] Q. Gillani, F. Ahmad, M. Mutalib, S. P. Melor, A. Arogundade. effect of dolomite clay on thermal performance and char morphology of expandable graphite based intumescent fire retardant coatings. Procedia Engineering 148 (2016) 146.

Tables

Due to technical limitations, table 1-3 is only available as a download in the Supplemental Files section.

Figures

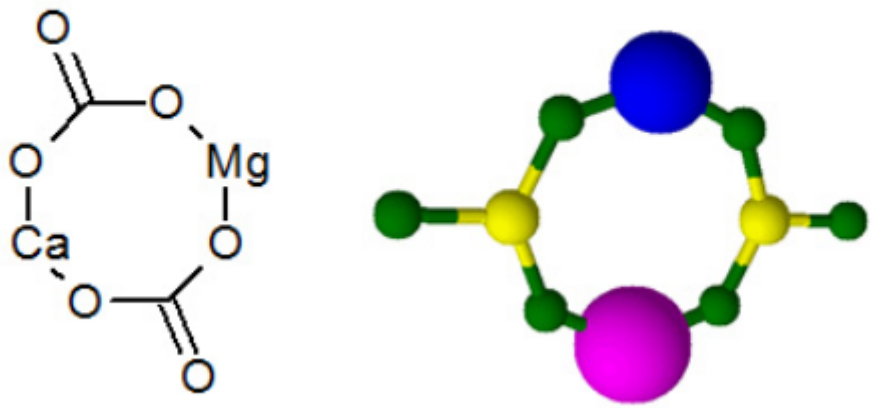

Figure 1

Structure of dolomite clay [29].

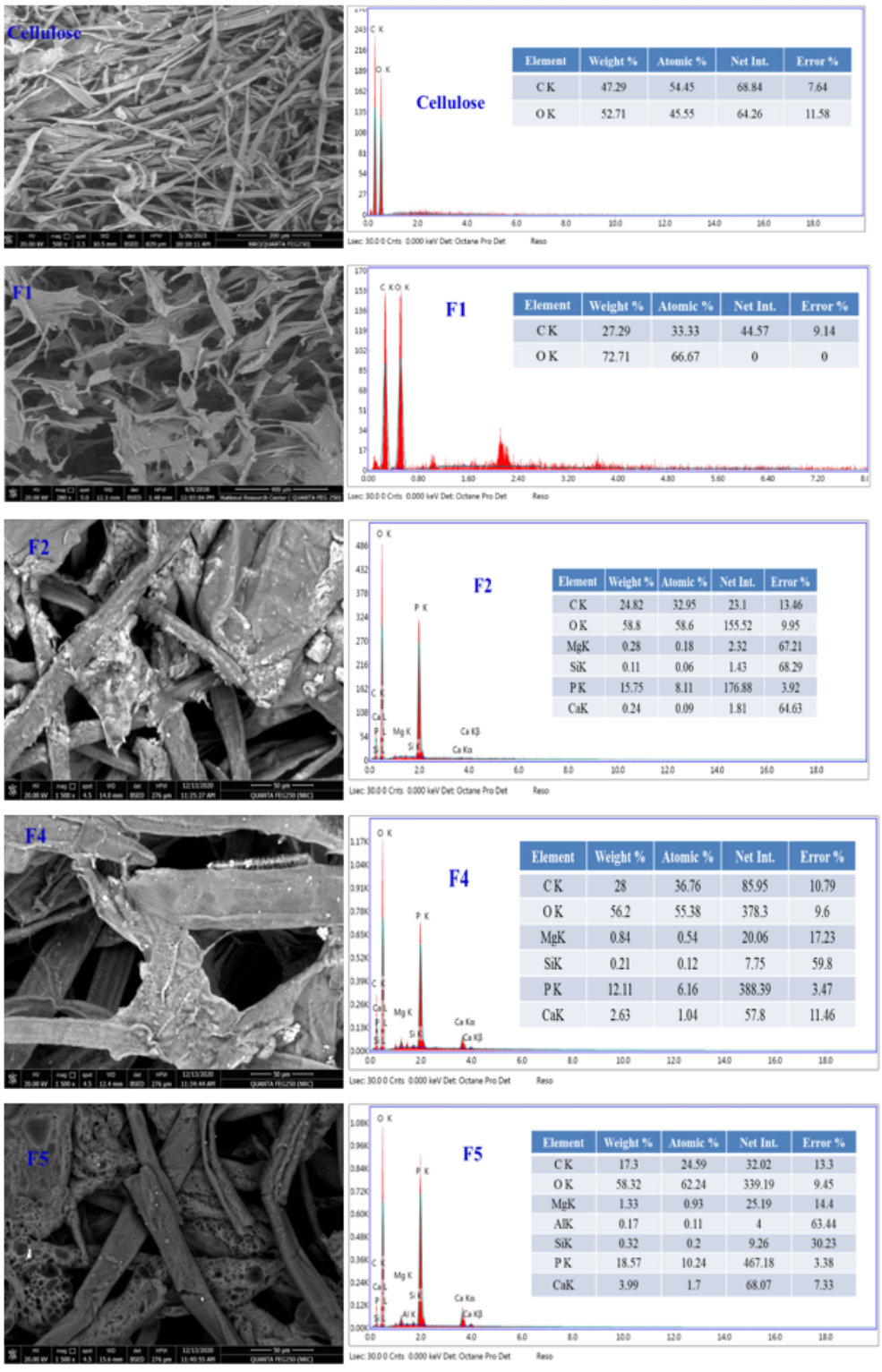

Figure 2

SEM images and EDX spectra of cellulose, activated cellulose and foams with different amounts of dolomite.

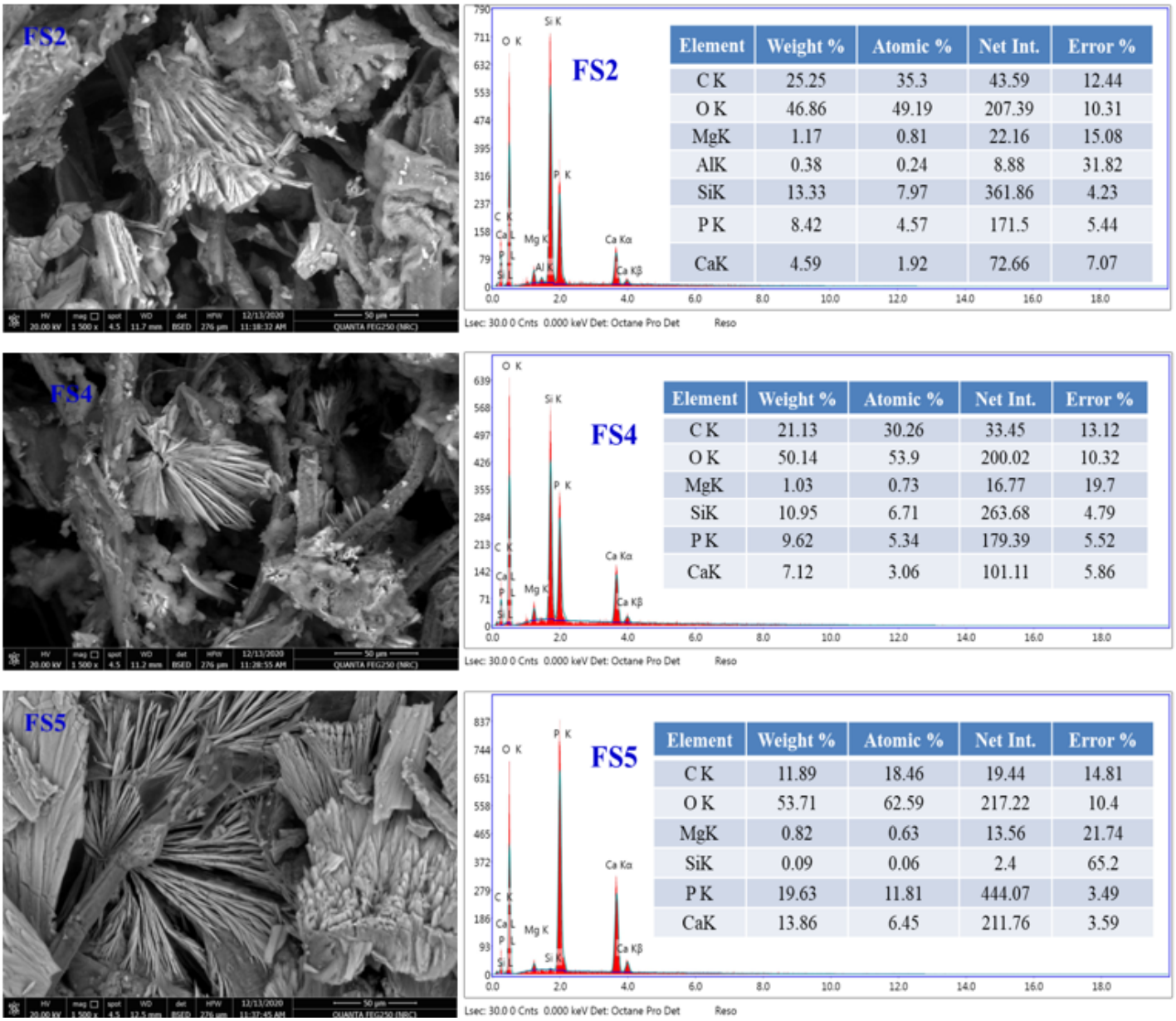

Figure 3

SEM images and EDX spectra of foam composite with silicone rubber with different amounts of dolomite.

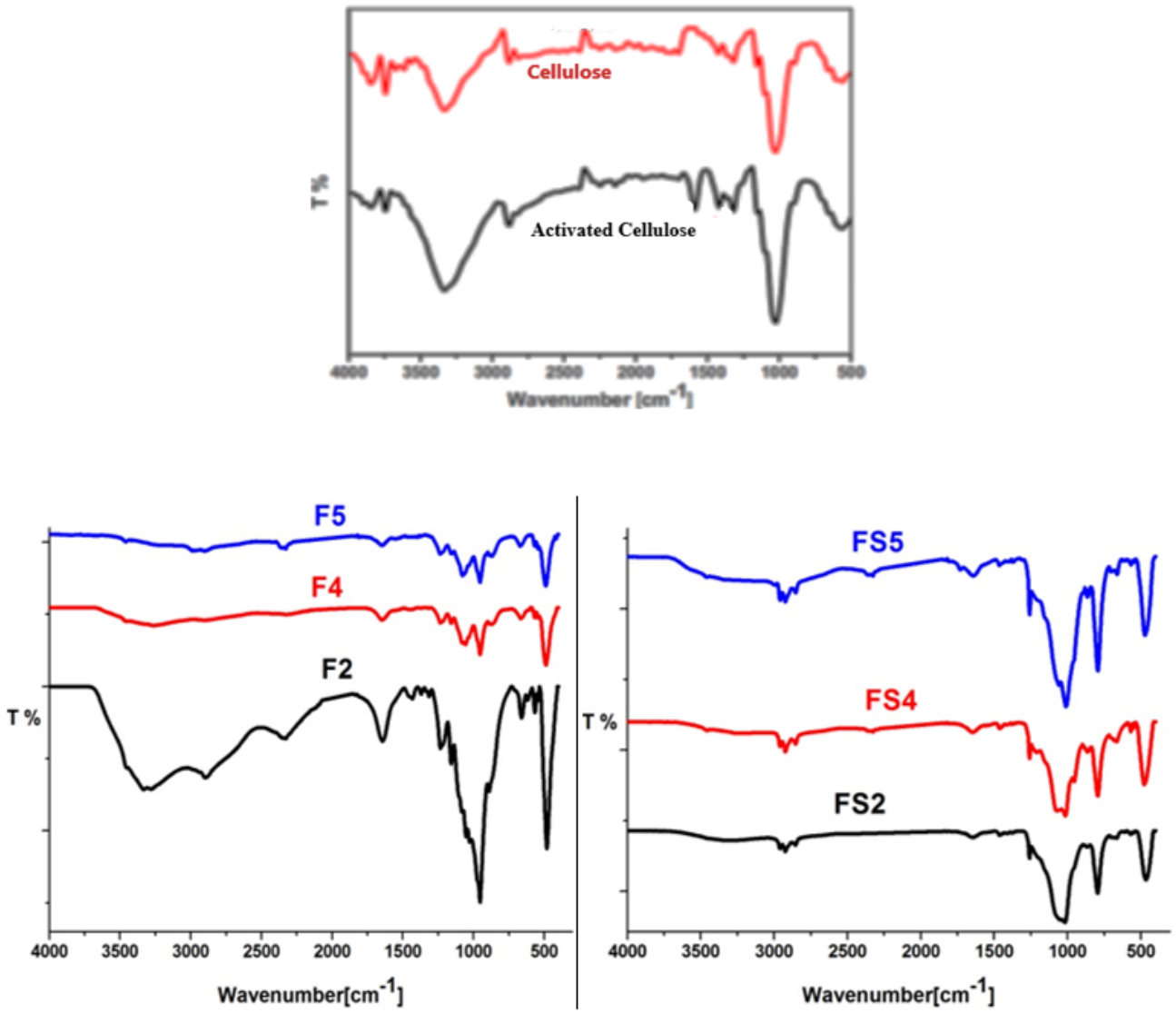

Figure 4

FTIR spectra of cellulose, activated cellulose and foams with different ratios of dolomite before (F2, F4, & F5) and after treatment with silicone rubber (FS2, FS4, & FS5).

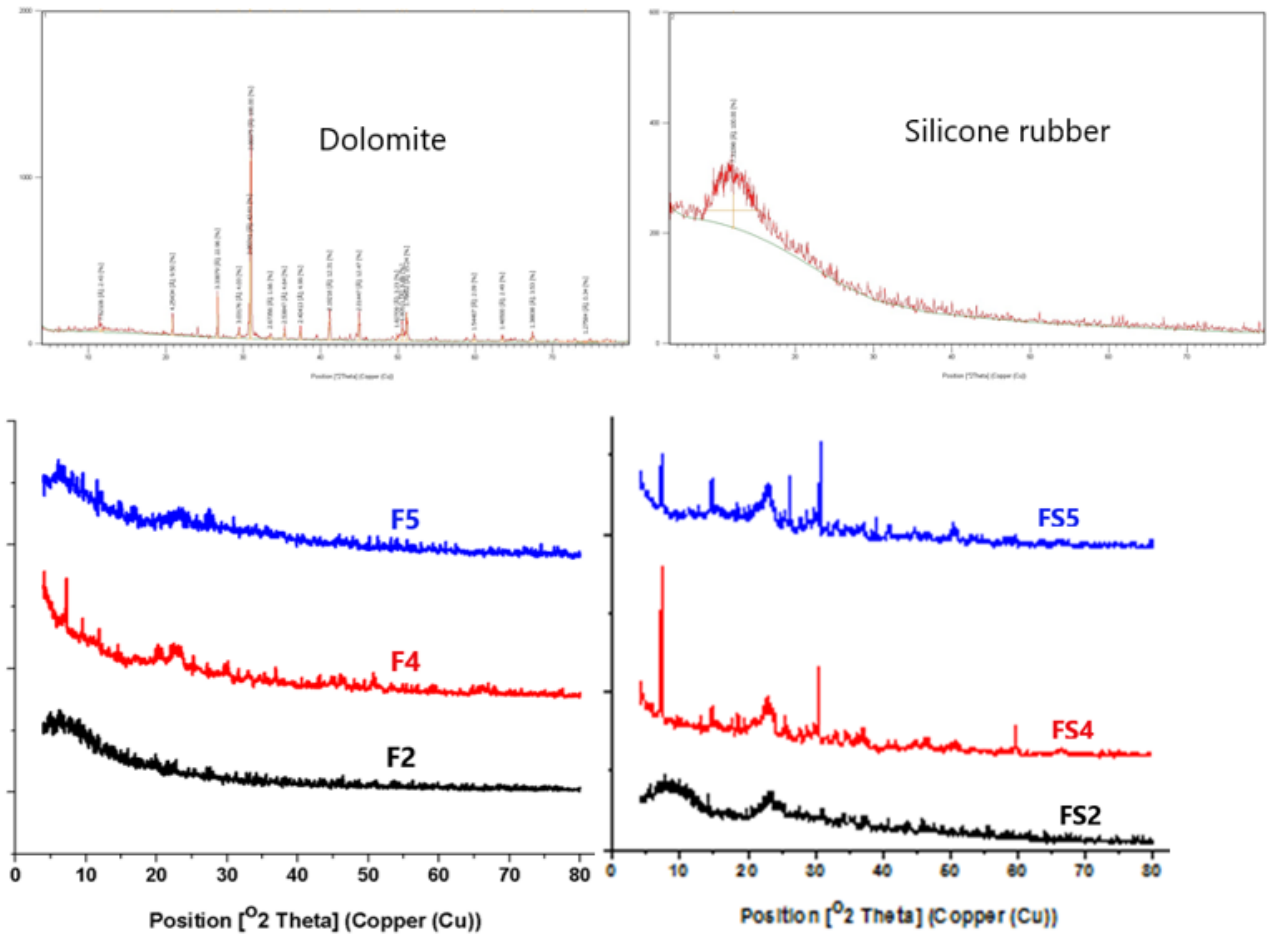

Figure 5

XRD patterns of dolomite, silicone rubber, and foams with different ratios of dolomite (F2, F4, & F5) and with silicone rubber (FS2, FS4, & FS5).

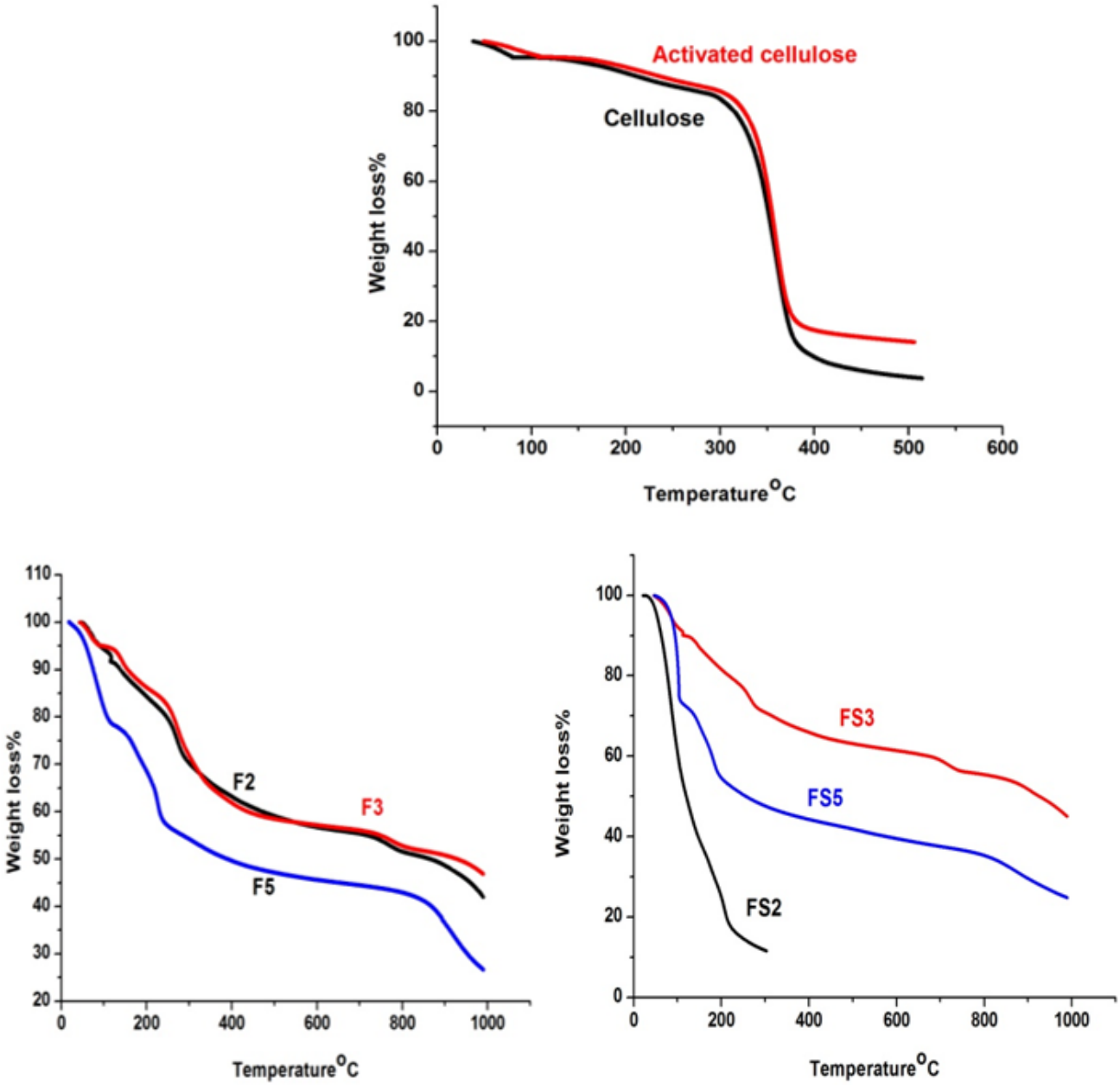

Figure 6

TGA of cellulose, activated cellulose and foams with different ratios of dolomite before and after treatment with silicone rubber.

Supplementary Files

This is a list of supplementary files associated with this preprint. Click to download.

- Tables.pdf